IJST, Transactions of Civil Engineering, Vol. 37, No. C2, pp 219-232
Printed in The Islamic Republic of Iran, 2013

EFFECT OF CONCRETE STRENGTH AND GROOVE DIMENSION ON PERFORMANCE OF GROOVING METHOD TO POSTPONE DEBONDING OF FRP SHEETS IN STRENGTHENED CONCRETE BEAMS*

D. MOSTOFINEJAD** AND M. J. HAJRASOULIHA

Dept. of Civil Engineering, Isfahan University of Technology (IUT), Isfahan, 84156-83111, I. R. of Iran
Email: dmostofi@cc.iut.ac.ir

Abstract– A major obstacle in using FRP sheets for flexural and shear strengthening has been debonding failure, which leads to premature and noneconomic failure of the strengthened element. Surface preparation of concrete member has been widely used to provide good bonding of the composite sheet onto concrete surface; however, it is found to be only partially effective in delaying debonding. Recently, Grooving Method (GM) has been introduced as a novel substitute for conventional surface preparation in Externally Bonded Reinforcement (EBR) strengthening of concrete beams. Although the previous experiments have shown that grooving method can postpone or even eliminate the debonding of FRP sheets from concrete substrate, the method is still in its early stages of development and awaits further research for maturation. The present study is an attempt to examine the effectiveness of grooving method for beams with different concrete compressive strength; also, to investigate the effects of groove depth and width on controlling FRP debonding for concrete specimens with different compression strengths.

The experimental specimens included 44 concrete beams, which with three samples per beam resulted in a total of 132 specimens. Initially, two grooves of varying widths and depths were made in each specimen. The grooves were then filled with an appropriate epoxy resin and the FRP sheets were bonded onto the concrete surface. After the resin had hardened, the specimens were subjected to the four-point flexural test. The experimental results showed the superiority of grooving method on conventional surface preparation for all four experimental categories with different compressive strength of concrete. The results also showed that a depth of 10 mm may be the optimum groove depth for all four experimental categories.

Keywords– Debonding, fiber reinforced polymer (FRP), grooving; RC beams, strengthening, surface preparation

1. INTRODUCTION

Structural strengthening nowadays poses a serious challenge to structural engineers. An array of methods are available for this purpose, the selection of which depends on a great number of variables; however, FRP composites have found wide applications in strengthening RC elements due to their unique properties such as high strength, low weight, ease of installation and corrosion resistance. The unique properties of FRP sheets have led to their widespread application in strengthening RC structures and RC joints covered with FRP overlays [1].

Flexural strengthening of reinforced concrete beams commonly involves bonding FRP sheets on the tensile side of the beam. Recent experimental researches have revealed that RC beams strengthened with plain FRP sheets undergo a variety of rupture modes. However, the rupture can be generally classified into the three types of flexural, shear, and debonding modes, and can be further divided into the following

*Received by the editors November 24, 2011; Accepted February 20, 2013.
**Corresponding author

groups [2]: a) flexural failure by FRP rupture, b) flexural failure by crushing of compressive concrete, c) shear failure, d) concrete cover separation, e) plate-end interfacial debonding, and f) intermediate flexural crack-induced interfacial debonding.

One important difficulty with RC beams strengthened with FRP sheets is their premature failure which is due to the sudden debonding of the sheet before its ultimate capacity can be exploited [3]. The most important cause of premature failure is the lack of an appropriate bonding interface between the FRP sheet and the concrete surface to achieve proper stress transfer between the two [4]. Accordingly, an important issue considered when using composites is the creation of an appropriate surface that allows for perfect bonding of the sheet onto the concrete surface. Concrete surface preparation is a common practice widely used for this purpose that enhances continuity and bond at the interface and delays the FRP sheet failure [5]. A special device is used in this method to scale a thin layer off the surface exposing the gravel in the concrete in order to create adequate bonding between the composite sheet and the concrete surface. Water or air jet is used to remove dust and the FRP sheet is then applied when the surface is completely dry [6]. Surface preparation of concrete, however, only partially delays debonding and sheet failure.

Over the past few years, numerous studies have been carried out to investigate the causes of debonding and to discover appropriate methods for delaying it. A brief review of some of these studies follows.

Chajes et al. studied the nature of the bonding interface between the composite sheet and the concrete surface. They investigated the effects of such parameters as concrete surface preparation, the type of resin used, and concrete strength on the bonding strength of the two surfaces. Their results revealed that surface preparation could enhance ultimate bonding strength by 3% to 10% [7].

Spadea et al. used one control beam and three beams of 140×300×5000 mm strengthened with CFRP at their tensile regions in their study and subjected them to the four-point flexural loading test. They tested their strengthened beams using displacement controlled procedure and measuring strains, displacement, and ultimate curvature. Their results revealed that it would not be possible to exploit the full capacity of the FRP sheet without the use of an external anchorage. They also found that external anchorage on the sheet not only led to 98.6% of its full capacity to be exploited but also its load carrying capacity to be enhanced by 70% as compared to the control beam. The application of an external anchorage in strengthening sheets also enhanced ductility of the beam by 25% to 45% compared to the control [8].

Toutanji and Ortiz prepared specimens in which they used a variety of FRP sheets. They also employed a variety of surface preparation methods such as water jet and sanding to investigate the effect of concrete surface type on its bonding to FRP sheets. Their results indicated that specimens roughened by water jet had bond strength of more than 50% compared to those roughened by regular sanding [9].

Galecki et al. investigated the effect of concrete surface hardness and roughness on its bond strength. They also experimented with water jet as a method for surface roughening. Their results indicated that when high-pressure water jet was used for surface preparation, bond strength was enhanced by 10% in the specimens without any other surface preparation [10].

Rosenboom and Rizkalla carried out a series of experiments to investigate the debonding of FRP sheets off the surface of beams strengthened with CFRP due to intermediate cracking. They used CFRP to strengthen 6 prestressed RC beam specimens 9.14 m long and subjected them to flexural loading. In their experiments, one beam experienced full rupture of FRP sheet and 4 experienced failure due to sheet debonding resulting from intermediate cracking. One beam was used without any strengthening as control to investigate the concrete crushing load of the beam. The results indicated that failure commonly occurs due to intermediate cracking (IC) in prestressed flexural members with long spans. They also found that U-shaped wraps applied after surface preparation to avoid premature failure increased the ultimate failure strength by 20% [11].

Ascione et al. investigated the stresses between the concrete beam and FRP sheets through FE analysis, and presented a new procedure to evaluate the peak value of longitudinal shear interactions to preserve FRP systems from premature debonding failure [12, 13]. Taheri et al. stated the hypothesis that the debonding of FRP sheets are a function of difference between Poisson's ratio of concrete and composites and as the difference between the two Poisson's ratios increases, debonding occurs faster [14].

Researchers have recently been motivated to direct their investigations toward finding substitute surface preparation methods that better deal with debonding phenomenon.

Over the last few years, near surface mounted (NSM) technique has been introduced as a valid alternative to externally bonded FRP laminates. In the NSM technique, grooves are first cut into the concrete cover of RC element, then FRP bars or strips are embedded in them using an appropriate binding agent such as epoxy resin or cement grout. Reduced risk of debonding is one of the main advantages of NSM method. Hajihashemi et al. investigated the cracking and ultimate loads of RC beams strengthened by prestressed FRP strips using NSM method; they reported 15% increase in the ultimate load and less cracking and deformation in the beam [15].

Mostofinejad and Mahmoudabadi commenced their series of experiments and developed grooving method (GM) to be used in Externally Bonded Reinforcement on Grooves (EBROG) strengthening technique as a novel substitute for the conventional surface preparation in Externally Bonded Reinforcement (EBR) strengthening method [16]. For their purposes, they constructed about 120 concrete beam specimens of 100×100×500 mm, which they categorized into 8 groups. Each group was subjected to the four-point flexural test to investigate one of their research objectives. A variety of groove types, such as longitudinal, transverse, and diagonal, were used as potential substitutes for the surface preparation practices commonly used and compared the obtained results. The experimental results obtained from applying this method on small specimens were of great value in that, in most cases grooving completely prevented the debonding of the sheet or delayed it to a great extent. The best results obtained for the specimens with longitudinal grooves of 10 mm deep, where the ultimate failure load rose by 80% as compared to the conventionally surface prepared specimens and debonding of FRP sheets from concrete substrate was fully eliminated.

Mostofinejad and Tabatabaei Kashani studied the effects of surface preparation on shear strengthening of RC beams; also the substitute of conventional surface preparation with grooving method is considered. Experimental specimens consisted of 32 small scale concrete beams which were subjected to 4-point loading test. The results revealed that the surface preparation of concrete can delay debonding even slightly and, accordingly, increase carrying loads of beams up to 12%. Furthermore, the results showed that grooving method performs better than surface preparation; so that the detachment of FRP strips did not occur in any of the beam specimens strengthened by this method and the weakness of beams in shear disappeared and flexural failure became dominant failure mode. [17].

Since Externally Bonded Reinforcement on Grooves (EBROG) is a novel method awaiting further research to mature, it is the objective of the present study to determine the effectiveness of grooving method on concrete with various compressive strengths; also, to investigate the effects of groove depth and width on FRP sheet debonding.

Below is a description of the stages of grooving on concrete surfaces [18]:

1. The relevant area of the concrete surface is marked for strengthening with FRP (Fig. 1a); then the area is marked with desirable spacing (e.g., 10 mm) for making longitudinal grooves (Fig. 1b).
2. Using an abrasive with an appropriate cutting plate, the marked grooves are cut to desirable widths and depths (Fig. 1c). Care must be taken in making deep longitudinal grooves of, say, 10 or 12.5 mm so that the depths are made in stages.

3. Once the grooves are made, air jet is used to clean the dirt and debris materials from them (Fig. 1d). After cleaning, the longitudinal grooves are filled with Epoxy Dur 31 N to obtain a smooth and even surface (Fig. 1e). Immediately after, another Epoxy resin, called Epoxy Dur 300, is used for bonding FRP sheets on the concrete surface.

(a)

(b)

(c)

(d)

(e)

Fig. 1. Creating grooves on concrete surface

2. SPECIMEN DETAILS AND MATERIAL CHARACTERISTICS

The specimens were used as beams with dimensions of 100×100×500 mm. Four different mixes were used in this study as detailed in Table 1. Super plasticizer with melamine formaldehyde base, and silica fume were used in making concrete specimens with high compressive strength. Limestone aggregates were used in making all four of the mixes used. The specimens were thus constructed and were removed from their molds after 24 hours and cured for 28 days in water according to ASTM C 192 [19]. Carbon fibers were used in the composite sheets utilized for flexural strengthening of the concrete beams. The fibers had a modulus of elasticity equal to 231 GPa, an ultimate tensile strength of 4100 MPa, a thickness of 0.12 mm, and an ultimate rupture strain of 1.7%.

Table 1 Concrete mix design

Strength category	Average compressive strength (MPa)	$(\frac{W}{C})$	Water (kg/m^3)	Cement (kg/m^3)	Coarse agg. (kg/m^3)	Fine agg. (kg/m^3)	Super plasticizer (kg/m^3)	Silica fume (kg/m^3)
1	30	0.61	228	374	736	996	-	-
2	45	0.47	228	485	736	867	-	-
3	62	0.40	159	398	1096	635	6.4	-
4	75	0.35	159	454	1094	584	8.8	71

3. TEST LAYOUT AND PROCEDURE

Each of the prism specimens was assigned to one of the four categories of compressive strength. Three depths of 7.5, 10, and 12.5 mm and three different widths of 4, 6, and 8 mm were used with each of the compressive strengths of 30, 45, 62, and 75 MPa. The number of grooves (2) and groove length (beam length) were the constants in all the specimens used in this study. Also, the free distance (face to face) of the grooves was constant and equal to 10 mm. In each compressive strength category, two controls were used: one concrete specimen without FRP strengthening and one both strengthened with CFRP and conventionally surface prepared. The specimens in each of the compressive strength categories were divided into 11 groups designated by A to K based on variations in groove depth and width. The details are presented in Table 2. It must be noted that group J includes the specimens without CFRP strengthening and the K group includes those strengthened with CFRP and conventionally surface prepared.

Table 2 Specification of the test specimens

Beam group	A	B	C	D	E	F	G	H	I	J	K
Groove width (mm)	4	4	4	6	6	6	8	8	8	N.A. (no strengthening)	N.A. (conventional surface prep.)
Groove depth (mm)	7.5	10	12.5	7.5	10	12.5	7.5	10	12.5		
Average compressive strength (MPa)											
f_c' = 30 MPa	28.25	30.39	31.05	29.20	29.20	28.89	30.12	30.12	28.89	28.25	28.89
f_c' = 45 MPa	44.92	44.92	45.49	45.14	45.14	45.14	45.86	46.11	44.43	44.92	44.92
f_c' = 62 MPa	63.49	62.22	62.22	60.78	60.78	60.78	62.81	61.71	61.71	63.49	63.49
f_c' = 75 MPa	75.93	74.29	74.29	73.38	73.38	73.38	76.89	75.23	75.23	75.93	75.93

As already explained above, one specimen was used as control in each of the compressive strength categories that was surface prepared using conventional methods. According to this method and as suggested by Hutchinson and Quinn, an abrasive is used to remove a surface layer of 2 to 3 mm from the concrete slurry [6]. After cleaning with an air jet, the pores created on the surface were filled with Epoxy Dur 31 N to obtain a smooth and even surface. Epoxy Dur 300 is then used to bond CFRP sheets on the surface.

The specimens thus constructed were subsequently subjected to the four-point flexural test under displacement control. Fig. 2 shows the machine used for the tests. To measure mid-span displacement in the specimens, 2 LVDTs were used on either side of the specimens and the load-displacement curves were plotted for further analysis.

Fig. 2. Test setup

4. RESULTS AND DISCUSSION

The load-groove width and load-groove depth curves were drawn for the beam specimens under flexural loading. The results are described and discussed as follows.

a) Test results for specimens in 30 MPa compressive strength category

The measured compressive strength of the specimens in this category was 30 MPa. These specimens exhibited the lowest cracking load among all the categories.

Figures 3a and 3b show load-groove depth and load-groove width curves for the specimens in this category. Ultimate loads in these figures are reported as the mean of ultimate loads of the specimens in one group.

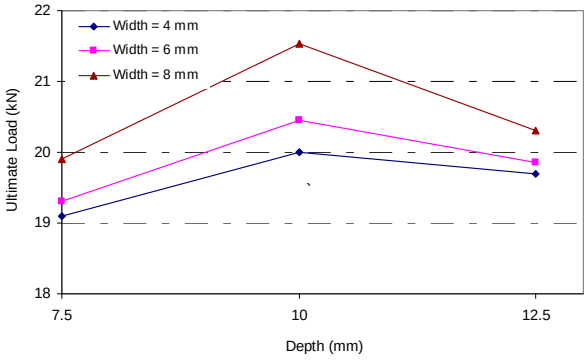

(a)

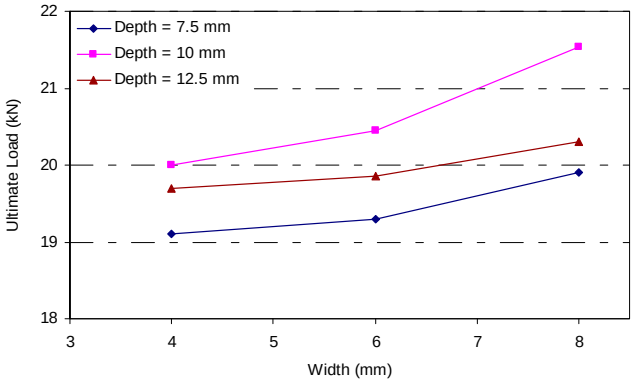

(b)

Fig. 3. Effect of groove dimension on loading capacity of beam specimens with f'c = 30 MPa; a) ultimate load versus groove depth; b) ultimate load versus groove width

As observed in Fig. 3a, the ultimate failure load of the sheets increased by around 4.7%, 5.9%, and 8.2%, respectively, for constant groove widths of 4, 6, and 8 mm when groove depth increased from 7.5 to 10 mm. With further increase in depth from 10 to 12.5 mm, however, the ultimate failure load of the sheet reduced by 1.5%, 2.9%, and 5.7%, respectively. This means that changes in groove depth for a width of 4 mm had a lower effect on the sheet ultimate failure load, but had a greater effect when width changed to 6 or 8 mm.

Inspection of Fig. 3a reveals that the depth of 10 mm is the optimum depth for all groove widths investigated because the highest failure load obtained for this depth. Increasing depth above 10 mm led to a disruption in load transfer from the concrete to the sheet, thus reducing the ultimate failure load of the sheet.

On the other hand, as seen in Fig. 3b, the ultimate failure load of the sheet increased by 1.0%, 2.2%, and 0.7% for groove depths of 7.5, 10, and 12.5 mm, respectively, with increasing groove width from 4 to 6 mm. Further increase in width from 6 to 8 mm, however, led to increased ultimate failure load of the sheet by 3.1%, 5.3%, and 2.3%, respectively.

It can be inferred from Fig. 3b that in this category, for each constant depth, increased groove width led to an increase in the ultimate failure load of the sheet with the highest value obtained for a width of 8 mm. Although increasing width to above 8 mm seems to have led to higher values of ultimate failure load due to the increased contact surface area between the sheet and the epoxy resin inside the groove, this required a greater cut in the surface of the concrete specimen, which in turn caused greater damage to the specimen and utilized excessive amounts of epoxy resin, which is neither economically nor practically justified.

Fig. 4 presents load-displacement curves for some of the specimens with a compressive strength of 30 MPa. Each curve represents the mean for identical specimens. Based on Fig. 4, it is clear that bonding of the FRP sheet using the conventional surface preparation methods leads to a 27% increase in the ultimate failure load of the specimen as compared to that of the specimen lacking flexural strengthening. This is while the ultimate failure load increases by a minimum of 19% and a maximum of 34% in specimens strengthened with FRP sheets bonded through grooving as compared to those conventionally surface prepared, as indicated in Figs. 3a and 3b.

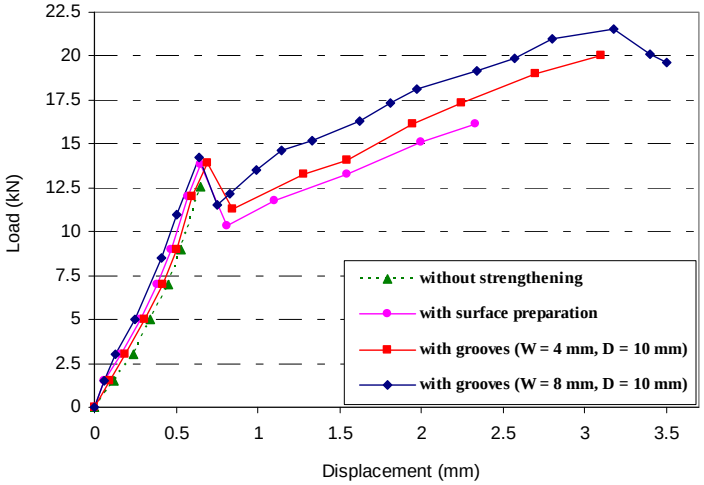

Fig. 4. Load-displacement curves for specimens with f'c = 30 MPa

b) Test results for specimens in 45 MPa compressive strength category

Figures 5a and 5b present load-groove depth and load-groove width curves for the 45 MPa strength

category. Increased cracking load in this category caused greater damage to the bonding of sheet and groove surface during cracking than what was observed in the previous category; the damage was higher for groove widths as low as 4 mm. This makes it impossible for stress to be completely transferred from the sheet to the concrete via the epoxy resin inside the 4 mm wide groove. Furthermore, it causes the change in depth to have only a slight effect on the ultimate failure load of the sheet at this width, as confirmed by the mild slope of the curve for the 4-mm width in Fig. 5a. The damage to the bonding between the sheet and the groove surface during cracking declined for widths of 6 and 8 mm with increasing contact area between the sheet and the epoxy resin inside the groove, which enhanced the transfer of stress via the epoxy resin inside the groove. Consequently, the effect of depth on the ultimate failure load increased at widths of 6 and 8 mm, as witnessed by the increased sloping of the curve for these widths.

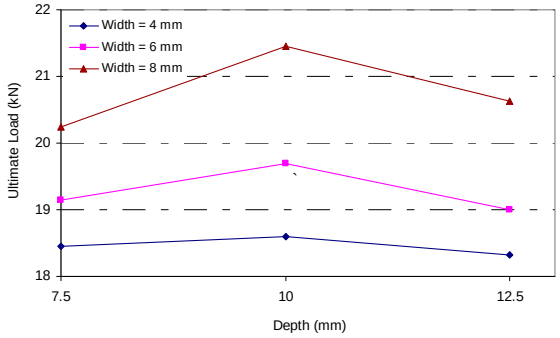

(a)

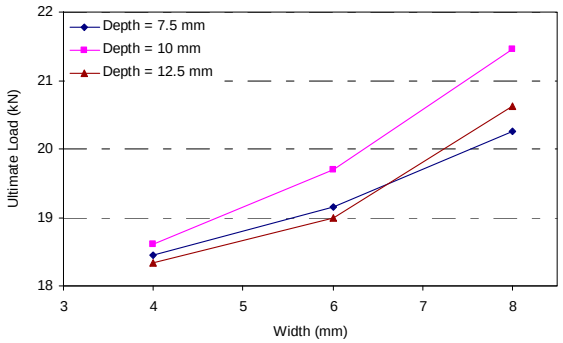

(b)

Fig. 5. Effect of groove dimension on loading capacity of beam specimens with f'c = 45 MPa; a) ultimate load versus groove depth; b) ultimate load versus groove width

Inspection of Fig. 5a reveals that at a compressive strength of 45 MPa and for constant widths of 4, 6, and 8 mm, the ultimate failure load of the sheet increased by 0.8%, 2.9%, and 5.9%, respectively, when groove depth increased from 7.5 mm to 10 mm. Further increase in depth from 10 to 12.5 mm, however, reduced this value by 1.5%, 3.6%, and 3.8%, respectively. Another finding obtained from examining Fig. 5a is that the optimum depth for all widths is 10 mm at which the highest sheet failure load was obtained.

It is clear from Fig. 5b that at constant groove depths of 7.5, 10, and 12.5 mm, sheet ultimate failure load increased by 3.8%, 5.9%, and 3.6%, respectively, when groove width increased from 4 to 6 mm. Further increase in width from 6 to 8 mm caused the ultimate failure load to increase again by 5.7%, 8.9%, and 8.6%, for groove depths of 7.5, 10 and 12.5 mm, respectively.

Figure 6 presents the load-displacement curves for some of the specimens with a compressive strength of 45 MPa. Based on Fig. 6, bonding of FRP sheets with conventional surface preparation led to a 17% increase in sheet ultimate failure load compared to the specimen without flexural strengthening. In

those specimens in this category in which the FRP sheet was bonded on the concrete surface via grooving, the ultimate failure load increased by a minimum of 7% and a maximum of 25% as compared to the case of conventional surface preparation. Clearly, grooving outperformed conventional surface preparation in this category, too. However, the percentage increase in ultimate failure load reduced in the specimens in this category compared to the specimens in strength category of $f_c^{'}$= 30 MPa; the most important reason for this can be contributed to the increased cracking load in the specimens leading to damage to bonding of the sheet onto the concrete surface at cracking and preventing the perfect load transfer to occur from the sheet to the concrete.

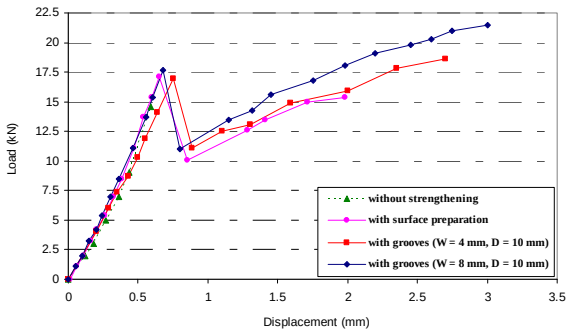

Fig. 6. Load-displacement curves for specimens with f'c = 45 MPa

c) Test results for specimens in high compressive strength category

The specimens in this category had the highest compressive strength among the test specimens; i.e. compressive strength of 62 or 75 MPa thus experienced the highest cracking load. Figures 7 and 8 present load-groove depth and load-groove width curves for these specimens.

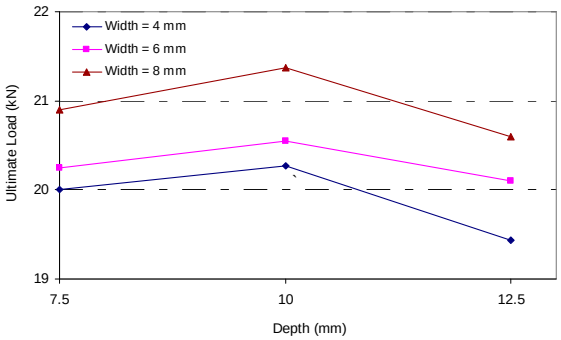

(a)

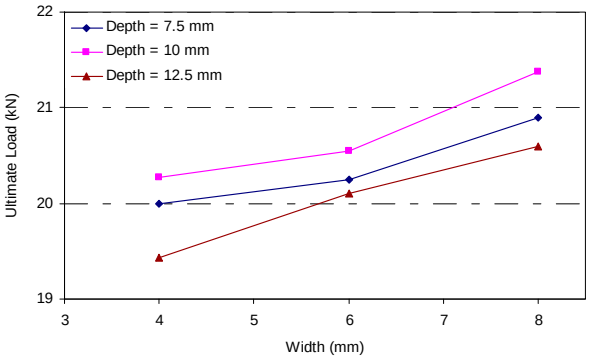

(b)

Fig. 7. Effect of groove dimension on loading capacity of beam specimens with f'c = 62 MPa; a) ultimate load versus groove depth; b) ultimate load versus groove width

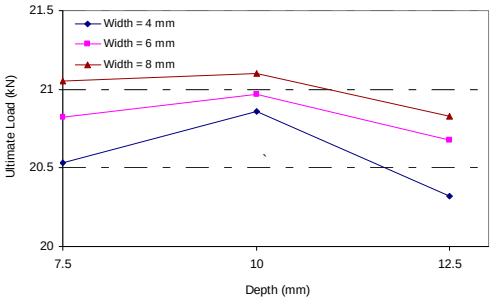

(a)

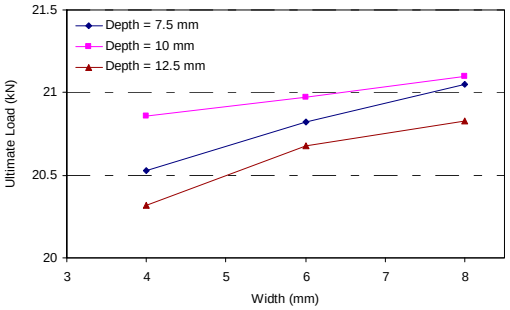

(b)

Fig. 8. Effect of groove dimension on loading capacity of beam specimens with f'c = 75 MPa; a) ultimate load versus groove depth; b) ultimate load versus groove width

Inspection of Figs. 7a and 8a reveals that the ultimate failure load of strengthened specimens increased slightly for constant groove widths of 4, 6, and 8 mm when the groove depth rose from 7.5 to 10 mm. Further increase in depth from 10 to 12.5 mm, however, led to reduced ultimate failure loads. Like in the other categories, a depth of 10 mm for all groove widths was found to be the optimal depth at which the highest failure load was obtained.

It is observed from Figs. 7b and 8b that the load-groove width curves are closer to each other with lower slopes, indicating that at high compressive strengths, increasing groove width has less effect on enhancement of the ultimate failure load of FRP sheet and postpone premature debonding. For instance, according to Fig. 7b, in compressive strength of 62 MPa, the ultimate failure load of the sheet increased by 1.2%, 1.4%, and 3.4% for constant depths of 7.5, 10, and 12.5 mm when groove width rose from 4 to 6 mm. When width further increased to 8 mm, the ultimate failure load also increased again by 3.2%, 4.0%, and 2.5% for the relevant groove depths. Like in the previous categories, at each constant depth, increasing width led to an increase in the ultimate failure load with its maximum value obtained for a depth of 8 mm.

Figs. 9 and 10 show the load-displacement curves for some of the specimens with the compressive strengths of 62 and 75 MPa.

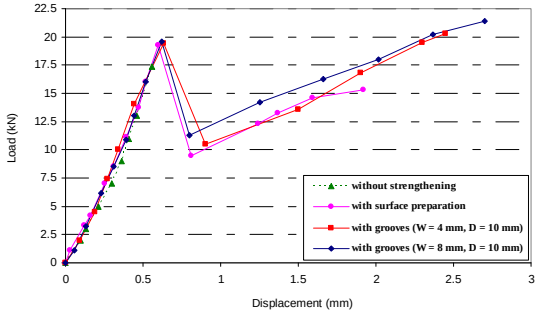

Fig. 9. Load-displacement curves for specimens with f'c = 62 MPa

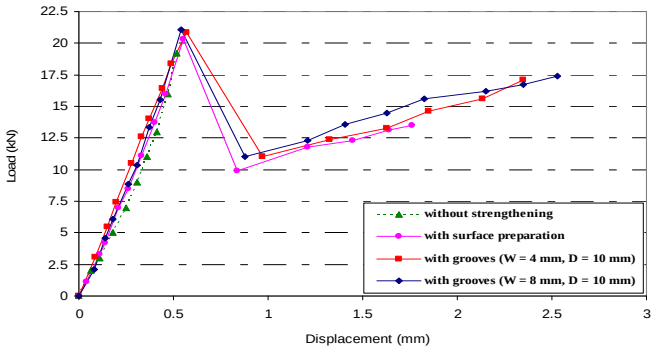

Fig. 10. Load-displacement curves for specimens with f'c = 75 MPa

In the high compressive strength category as in other categories, grooving outperformed conventional surface preparation; however, the percentage increase in the ultimate failure load was lower in this category than in those with lower compressive strengths, as shown in Figs. 9 and 10. To explain this, one may refer to the high cracking load in the category with compressive strengths of 62 and 75MPa causing serious damage and seriously weak bonding between the FRP sheet and concrete surface during cracking, which ultimately leads to the premature debonding of portions of the sheet at cracking point. This premature debonding reduces the ultimate load capacity of the FRP sheet.

d) Load-displacement curves at various compressive strengths

Comparison of load-displacement curves indicates an identical linear behavior among the curves for the specimens in each category prior to a tangible reduction occuring in load due to cracking. After cracking and the consequent considerable reduction in load, the curves show different patterns in their behavior depending on the type of surface preparation (conventional or with grooving) method. It is interesting to note that the curve slope declines after cracking compared to its linear slope prior to cracking; which, in fact, is stiffness degradation due to failure of concrete in tension zone after cracking. These curves also reveal that, in addition to increased ultimate failure strength, the flexural strengthening of the beams increases their ductility and cracking load. The total area under the load-displacement curve represents the amount of energy absorbed by the strengthened specimens at the time of failure. The surface areas under the load-displacement curves for some of the strengthened specimens are computed and presented in Table 3.

Table 3. Area under load-displacement curves

Average compressive strength (MPa)	Beam group	Area under the curve (N.mm×10^3)	Increase in the area (%)
30	K	128	-
	B	247	93
	H	535	318
45	K	137	-
	B	222	62
	H	428	212
62	K	122	-
	B	182	49
	H	221	81
75	K	119	-
	B	168	41
	H	211	77

Based on the data presented in Table 3, creating grooves 4 mm wide and 10 mm deep in specimens with compressive strengths of 30, 45, 62, and 75 MPa, respectively, led to enhanced areas under the load-displacement curves by 93%, 62%, 49%, and 41%; however, grooves 8 mm wide and 10 mm deep led to even greater increases of 3.5 times, for strength categories of 30 and 45 MPa, and over 3 times, and nearly 2 times, respectively, for strength of 62 and 75 MPa, compared to those for specimens with conventional surface preparation. This indicates that grooving increases the area under the load-displacement curve in the specimens of all the test compressive strength categories when compared to those simply prepared by conventional methods. Moreover, ductility and energy absorption is higher in the grooved specimens. However, when compressive strength increases, the efficiency of grooving approaches that of plain surface preparation. Another interesting point to note is that by increasing groove width from 4 to 8 mm in each of the categories, energy absorption capacity rises by over 2 times, 3 times, over 1.5 times, and nearly 2 times for the strength categories of 30, 45, 62 and 75 MPa, respectively; which indicates the considerable effect of increasing groove width on enhancing ductility.

e) Failure modes in specimens with different compressive strengths

Failure types observed in the specimens with different compressive strengths are presented in Table 4. For each category, the table shows the number of specimens in which the sheet has undergone complete rupture (Fig. 11a), partial rupture and partial debonding (Fig. 11b), or complete debonding (Fig. 11c). Evidently, complete rupture together with flexural failure is observed in most specimens with a compressive strength of 30 MPa, indicating the good performance of grooving method in this category. The number of specimens experiencing complete rupture of their FRP sheet reduced when the cracking load increased at higher compressive strengths. This has a direct relationship with the high cracking load during cracking, where part of the sheet outside the groove area detaches intact from the concrete surface during loading, which causes a drastic drop in the ultimate capacity of the sheet. At high compressive strengths of concrete of 62 and 75 MPa, creating grooves as small as 4 mm wide led to complete debonding of the sheet off the concrete surface during initial cracking. This is due to the fact that, at high compressive strengths, small grooves lack the ability to transfer loads between the sheet and the concrete and, hence, the sheet undergoes premature debonding.

Table 4. Observed modes of failure for different strength categories

Category No.	Average compressive strength (MPa)	Total number of strengthened specimens	Failure mode		
			Full rupture of FRP	Rupture-debonding of FRP	Debonding of FRP
1	30	26	19	4	3
2	45	32	15	14	3
3	62	29	3	25	1
4	75	29	1	26	2

(a) (b) (c)

Fig. 11. Failure mechanisms of strengthened specimens ; a) FRP full rupture; b) rupture-debonding of FRP; c) debonding of FRP

5. SUMMARY AND CONCLUSIONS

The present study investigated the effects of compressive strength of concrete as well as increasing groove depth and width on ultimate failure load in concrete beam specimens strengthened with FRP sheets using the recommended EBROG technique. 132 concrete beam specimens with a dimension of 100×100×500 mm were constructed and subjected to the four-point flexural test. The specimens were sorted into four categories according to their compressive strength. Grooves with combinations of three different widths of 4, 6, and 8 mm and three different depths of 7.5, 10, and 12.5 mm were created in the specimens; then the specimens were strengthened with FRP sheets and subjected to the four-point flexural test. The results obtained from the current study can be summarized as follows.

1. In specimens with compressive strengths of 30 and 45 MPa, increase of groove depth increased the ultimate flexural failure load of the beams, although in the specimens with a groove width of 4 mm, the effect of groove depth on the ultimate failure load was far lower than that due to groove widths of 6 and 8 mm. However, in specimens with compressive strengths of 62 and 75 MPa, increasing depth had a limited effect on the ultimate failure load for all groove widths of 4, 6, and 8 mm.
2. A depth of 10 mm was found to be the optimum depth for all groove widths as it yielded the highest sheet failure load.
3. In all the test categories of compressive strength, for each constant depth (7.5, 10, and 12.5 mm), increasing groove width increased the ultimate failure load. At all depths and in specimens with compressive strengths of 62 and 75 MPa, the load-groove width curves were closer to each other compared to corresponding curves for the specimens with compressive strengths of 30 and 45 MPa, due to the reduced effect of increasing groove depth at each constant width.
4. In most strengthened specimens with a compressive strength of 30 MPa, complete FRP debonding was observed accompanied by flexural failure. However, in specimens with a compressive strength of 45 MPa, complete rupture of the FRP sheet occurred only for 6 and 8 mm widths. In specimens with compressive strengths of 62 and 75 MPa, the most frequent failure was partial rupture and partial debonding of FRP sheets, while complete rupture occurred in only a few specimens.
5. Compared to the conventional surface preparation methods, the grooving method introduced for EBROG strengthening technique increased the area under the load-displacement curve in all four test categories. This evidences that energy absorption is higher in grooved specimens strengthened with FRP than that in those strengthened with FRP but conventionally surface prepared. It is interesting to note that the highest energy absorption in grooved specimens was observed in those with a compressive strength of 30 MPa while the lowest was observed in those with a compressive strength of 75 MPa.

REFERENCES

1. Mostofinejad, D. & Talaeitaba, S. B. (2006). Finite element modeling of RC connections strengthened with FRP laminates. *Iranian Journal of Science & Technology, Transaction B: Engineering*, Vol. 30, No. B1, pp. 21-30.
2. Oehlers, D. J. (2001). Development of design rules for retrofitting by adhesive bonding or bolting either FRP or steel plates to RC beams or slabs in bridges and building. Composites: Part A, Vol. 32, pp. 1345-1355.
3. Teng, J. G., Chen, J. F., Smith, S. T. & Lam, L. (2002). FRP-Strengthened RC Structures. Wiley and Sons: England.
4. Karbhari, V. M. & Zhao, L. (1997). Issues related to composite plating and environmental exposure effects on composite-concrete interface in external strengthening. *Composite Structures*, Vol. 40, No. 3, pp. 293-304.
5. Mostofinejad, D. & Mahmoudabadi, E. (2009). Effect of elimination of concrete surface preparation on the

debonding of FRP laminates. *Concrete Solutions Conf*. Italy, pp. 357-361.

6. Hutchinson, A. R. & Quinn, J. (1999). *Strengthening of reinforced concrete structures.* Woodhead Publishing Limited, Cambridge, pp. 46-82.
7. Chajes, M. J., Finch, W. W., Januszka, T. F. & Thomson, T. A. (1996). Bond and force transfer of composite material plates bonded to concrete. *ACI Structural Journal*, Vol. 93, No. 2, pp. 208-217.
8. Spadea, G., Bencardino, F. & Swamy, R. N. (1998). Structural behavior of composite RC beams with externally bonded CFRP. *Journal of Composites for Construction*, Vol. 2, No. 3, pp. 132-137.
9. Toutanji, H. & Ortiz, G. (2001). The effect of surface preparation on the bond interface between FRP sheets and concrete members. *Journal of Composite Structures*, Vol. 53, pp. 457-462.
10. Galecki, G., Maerz, N., Nanni, A. & Myers, J. (2001). Limitation to use of waterjets in concrete substrate preparation. *Proc. American Waterjet Conference*, WJTA, Minneapolis.
11. Rosenboom, O. & Rizkalla, S. (2008). Experimental study of intermediate crack debonding in fiber-reinforced polymer strengthened beams. *ACI Structural Journal*, Vol. 105, No. 1, pp. 41-50.
12. Ascione, L. & Feo, L. (2000). Modeling of composite/concrete interface of RC beams strengthened with composite laminates. *Composites: Part B*, Vol. 31, pp. 535–540.
13. Ascione, L., Berardi, V. P., Feo, L. & Mancusi, G. (2005). A numerical evaluation of the interlaminar stress state in externally FRP plated RC beams. *Composites: Part B*, Vol. 36, pp. 83–90.
14. Taheri, F., Shahin, K. & Widiarsa, I. (2002). On the parameters influencing the performance of reinforced concrete beams strengthened with FRP plates. *Compos Struct*, Vol. 58, pp. 217–26.
15. Hajihashemi, A., Mostofinejad, D. & Azhari, M. (2011). Investigation of RC beams strengthened with prestressed NSM CFRP laminates. *ASCE, Journal of Composites for Construction*, Vol. 15, No. 6, pp. 887–895.
16. Mostofinejad, D. & Mahmoudabadi, E. (2010). Grooving as alternative method of surface preparation to postpone debonding of FRP laminates in concrete beams. *ASCE, Journal of Composites for Construction*, Vol. 14, No. 6, pp. 804-811.
17. Mostofinejad, D. & Tabatabaei Kashani, A. (2012). Experimental study on effect of EBR and EBROG methods on debonding of FRP sheets used for shear strengthening of RC beams. *Composites: Part B*, Vol. 45, No. 1, pp. 1704-1713.
18. Mahmoudabadi, E. & Mostofinejad, D. (2009). An alternative method to Surface preparation to postpone debonding of FRP laminates. *9th International Symposium of Fiber Reinforced Polymer Reinforcement for Concrete Structures*. Sydney: Australia.
19. American Society for Testing and Materials, (1997). Standard practice for making and curing concrete test specimens in the laboratory. ASTM C192-95; V.04.02; November.